Journal of Materials Chemistry A

ROYAL SOCIETY OF CHEMISTRY

PAPER

View Article Online
View Journal | View Issue

Cite this: J. Mater. Chem. A, 2023, 11, 21231

Fully recyclable high-performance polyacylsemicarbazide/carbon fiber composites†

Zhiwen Jian, Yindong Wang, Xiaokang Zhang, Xi Yang, Zhanhua Wang, Xili Lu* and Hesheng Xia *

Received 28th March 2023
Accepted 6th September 2023

DOI: 10.1039/d3ta01841e

rsc.li/materials-a

Realizing the complete and non-destructive recycling of carbon fiber reinforced composite materials is of great significance for the pursuit of sustainability and a circular economy. Although the application of resins containing dynamic bonds in carbon fiber composite materials has made great progress in recent years, the development of a completely recyclable resin matrix with high strength, high modulus, and high T_g is still a huge challenge due to the mutual exclusion of the dynamic properties and mechanical properties of the material. Here we report a novel dynamic polyacylsemicarbazide (PASC) material with ultra-high strength and modulus containing supramolecular multiple hydrogen bonding between the polymer chains. The influence of different chemical structures on the intermolecular hydrogen bond structure of the material is studied. The optimized PASC material with a Young's modulus of 4.1 GPa, a stress at break of 97.6 MPa, and a glass transition temperature (T_g) of 174 °C exhibits great reprocessing properties, excellent solvent recycling ability, and excellent water resistance. Furthermore, using this newly developed PASC material as the matrix resin, the carbon fiber reinforced polymer composite was successfully prepared through solution impregnation and thermal pressing. The composite material shows an optimized inter-layer shear strength of 36.7 MPa and a healing efficiency of 70.6%. The great dynamic and reversible characteristics of the material enable nearly 100% completely non-destructive solvent recycling of the carbon fiber and matrix resin, and the regenerated composite material still retains 82.3% of its initial inter-layer shear strength.

1. Introduction

Carbon fiber reinforced polymer composites (CFRPs) are widely used in aerospace and automotive industries due to their light weight and high strength.[1,2] The excellent properties of carbon fiber composite materials have made their global demand increase year by year, with an annual growth rate of 11.5%. By 2025, the global demand for carbon fibers will increase to 285 000 tons.[3,4] As the global consumption of carbon fiber composites increases, it also brings enormous economic and environmental challenges due to the limitation of service life and failure of composite materials. As early as the 1990s, some recycling methods for carbon fiber composites were studied, such as mechanical recycling, thermal or chemical degradation, *etc.*[5,6] However, these methods often require harsh recycling conditions such as high temperature and strong acid/alkali, and it is difficult to recycle the carbon fibers completely or non-destructively.[3,7] Meanwhile, the resin matrix of the traditional carbon fiber composites is often thermosetting, which cannot be recycled due to the infusible and insoluble characteristics of the cross-linked network. Therefore, the recycling of CFs and resins from carbon fiber reinforced composites in an efficient and non-destructive way remains a challenge.

Dynamic covalently cross-linked polymers, also known as a covalent adaptive network (CAN), are a class of resins containing dynamic chemical bonds in the polymer network. Such materials break the boundaries between traditional thermoplastic polymers and thermosetting polymers and possess outstanding advantages such as self-healing, reprocessing, recyclability, and configuration remodeling.[8] In recent years, the introduction of dynamic covalent bonds into carbon fiber composite has become an effective strategy to improve the recycling of carbon fiber composites. Various dynamic bonds such as an ester bond,[9–14] boronic ester bond,[15] Schiff base,[16–20] diselenide bond,[21] carbonate bond,[22] acetal bond,[23] urethane bonds,[24] disulfide bond[25,26] and Diels–Alder bond[27–30] have been introduced into the chemical structure of polymers (like epoxy, polyamide, polyurethane, *etc.*) to prepare a series of recyclable carbon fiber reinforced composites. Due to the reversible characteristics of these dynamic bonds under external stimuli (such as light, heat, pH, *etc.*), the self-healing and recycling of the composites can be realized. Although these strategies have achieved some good results, most of these dynamic polymers

State Key Laboratory of Polymer Materials Engineering, Polymer Research Institute, Sichuan University, Chengdu, 610065, China. E-mail: xililu@scu.edu.cn; xiahs@scu.edu.cn

† Electronic supplementary information (ESI) available. See DOI: https://doi.org/10.1039/d3ta01841e

are still some distance away from real industry applications due to some inadequacies including thermal stability, water resistance, catalyst solubility, aging resistance, complex preparation process, high cost, *etc.* Meanwhile, although the introduction of dynamic bonds improves the dynamic properties of the resin, the mechanical properties of the materials tend to decrease, because the dynamic properties and mechanical properties of the polymers are usually mutually exclusive.[31] Therefore, it is of great significance to prepare a dynamic resin matrix for carbon fiber reinforced composites with high strength, good heat resistance, and water resistance.

In our previous work, we first proposed the synergistic effect of the dynamic covalent bonds of acylsemicarbazide (ASC) moieties and their internal hydrogen bonds, and the polymer materials containing ASC moieties possessed a Young's modulus of up to 1.7 GPa and tensile strength of 68.5 MPa.[32] Subsequently, based on the ASC moieties, we prepared polyacylsemicarbazide with a Young's modulus of 2.8 GPa, a stress at break of 100 MPa, and a T_g of 123 °C by reacting adipic hydrazide (ADH) with 4,4′-methylenebis(cyclohexyl isocyanate) (HMDI), and also prepared their carbon fiber reinforced composites that showed excellent mechanical and healing performance.[33] However, there are still some challenges in further improving the mechanical properties, heat resistance, water resistance, and solvent recycling ability of the polymer matrix. Herein, we systematically studied the effect of different isocyanates on the internal hydrogen bond structure of PASC and selected IPDI, IPDH, and tri-HDI to prepare cross-linked PASC materials with ultra-high Young's modulus, solvent recycling ability, and water resistance. Then, the optimized PASC was selected as the resin matrix to prepare the carbon fiber composite, and the effect of the resin content on the performance of the composite material was investigated. Finally, the carbon fibers and matrix resins in the multilayered composites were successfully recycled by using a solvent without destruction.

2. Experimental

2.1 Materials

Isophthalic dihydrazide (IPDH, TCI, 95.0%), adipylhydrazide (ADH, TCI), hexamethylene diisocyanate trimer (tri-HDI, Bayer, Desmodur N3300), isophorone diisocyanate (IPDI, Adamas, 99%), 4,4′-methylenebis(cyclohexyl isocyanate) (HMDI, TCI, >90%, mixture of isomers), 1,6-diisocyanatohexane (HDI, Adamas, 98%), 4,4′-diphenylmethane diisocyanate (MDI, Adamas, 95%), cyclohexyl isocyanate (CHI, TCI, >98%), benzoylhydrazide (TCI, >98%), 4-methoxybenzoylhydrazide (TCI, >98%), *N*,*N*-dimethylformamide (DMF, Adamas, 99.5%, water #50 ppm), dimethyl sulfoxide (DMSO, Chron Chemicals), tetrahydrofuran (THF, Chron Chemicals), acetone (AC, Chron Chemicals), and ethanol absolute (Chron Chemicals) were used as received. The carbon fiber used in this study was 2/2 twill-weave carbon fabric (ZF-H03P-280) obtained from GuangWei Composites in China.

2.2 Characterization methods

Nuclear magnetic resonance (NMR) spectra were recorded at room temperature with a Bruker spectrometer operating at 400 MHz using DMSO-d6 as the solvent. Molecular weights were measured by gel permeation chromatography (GPC, TOSOH, HLC-8320 GPC) with DMF as the eluent at a flow rate of 0.6 mL min^{-1} at 40 °C. Raman spectra were measured using an inVia-Reflex Raman spectrometer (Renishaw, England) with a laser at 532 nm wavelength, 60 s exposure time, and 12 mW laser energy. X-ray diffraction (XRD) analysis was performed using an X-ray diffractometer (Empyrean) equipped with a Cu-Kα source and operated at 40 kV and 40 mA in the 2θ range of 10° to 60°. Fourier transform infrared spectroscopy (FTIR) analysis of the samples was performed on a Nicolet 560 FTIR spectrometer, with a diamond attenuated total reflection (ATR) attachment for ATR-FTIR. X-ray photoelectron spectroscopy (XPS) analysis was performed on a Thermo Scientific K-Alpha. Emission scanning electron microscopy (SEM) was performed on an FEI-Quanta 250 field instrument at an acceleration voltage of 20 kV. Tensile experiments were conducted on an Instron 5567 equipped with a 1 kN load cell at RT (25 °C) with a strain rate of 50 mm min^{-1}, and dumbbell shaped tensile bars were used (*ca.* 0.5 mm (T) × 3 mm (W) × 35 mm (L) and a gauge length of 15 mm). Tensile samples of CFRP prepregs with dimensions of 100 mm (L) × 10 mm × 0.5 mm were tested on an Instron 5567 equipped with a 10 kN load cell. The gauge length was 20 mm. The strain rate was 5 mm min^{-1}. At least three samples of each loading fraction were tested. The flexural properties of a two-layer CFRP laminate were tested on an Instron 5567 equipped with a 10 kN load cell. The sample size was 25 mm (L) × 10 cm (W). The thickness of each sample was measured using a digital caliper with 0.01 mm precision. The support span was 50.8 mm. At least three samples of each loaded section were tested. According to ASTM D2344, short beam shear (SBS) testing was conducted on an Instron 5567 equipped with a 10 kN load cell with a support span of 25 mm. The rate of crosshead motion was 1 mm min^{-1}. At least three samples of each loading fraction were tested and the reported results were average values. The thickness of each sample was measured using digital calipers as mentioned above. Dynamic mechanical analysis (DMA) was carried out on a DMA Q800 apparatus (TA Instrument) in tension film mode. Rectangular geometry samples (*ca.* 0.5 mm (T) × 3 mm (W) × 20 mm (L) and a gauge length of 8 mm) were characterized from 30 °C to 200 °C at a heating rate of 3 °C min^{-1}, a strain of 0.1% and a frequency of 1 Hz. Stress-relaxation analysis (SRA) was performed in tensile geometry on a DMA Q800 apparatus (TA Instrument), and rectangular samples were utilized (*ca.* 0.5 mm (T) × 3 mm (W) × 20 mm (L) and a gauge length of 8 mm). The samples were equilibrated at a set temperature for 5 min and then subjected to a constant strain of 1%. Creep analysis was performed in tensile geometry on the DMA Q800 apparatus (TA Instrument), and rectangular samples were utilized (*ca.* 0.5 mm (T) × 3 mm (W) × 20 mm (L) and a gauge length of 8 mm). The samples were equilibrated at a set temperature for 5 min and then stretched for 10 min under a constant stress of 5 MPa. After that, the stress is released and the sample is restored at the same temperature for another 20 min to record the change in strain over time during the entire process.

2.3 Synthesis processes of PASC

The synthesis process of PASC is similar to that in our previous work.[32,33] Fig. 1a shows the chemical structure of linear PASC materials prepared from different isocyanates. Specifically, IPDH was first added to DMF, and equimolar isocyanate was added under vigorous stirring, and the stirring was continued until the cloudy solution became clear. Then the solution was defoamed to remove air bubbles in the solution, poured into a mold, dried at 80 °C for 48 h, and then heated to 100 °C and dried in a vacuum environment for 48 h to obtain a uniform material.

The preparation method of the cross-linked PASC material is similar to that above, as shown in Fig. 3a. Specifically, a certain amount of IPDH is first added to DMF, and a suspension is formed under vigorous stirring. Then, a certain amount of IPDI and the cross-linking agent tri-HDI were added with stirring, and stirring was continued until the cloudy solution became clear. Then the solution was defoamed to remove air bubbles in the solution, poured into a mold, dried at 80 °C for 48 h, and then heated to 100 °C and dried in a vacuum environment for 48 h to obtain a uniform material. The crosslinking index is defined as the molar percentage of isocyanates in tri-HDI as a total isocyanate. The condition for isophthalamide to cure E51 epoxy resin is to cure at a constant temperature of 80 °C for 2 h, and then cure at 100 °C for 2 h.

2.4 Water resistance test of PASC materials with different isocyanates

The water resistance test at room temperature (RT): dumbbell-shaped tensile splines (0.5 mm (T) × 2 mm (W) × 35 mm (L)) of PASC materials prepared with different isocyanates were immersed in deionized water for 30 days at RT. Then the sample was taken out, the water on the surface of the sample was wiped off, and then the tensile test of the samples was carried out with a tensile rate of 50 mm min^{-1}.

GB T 2573-2008 was used to characterize the high temperature water resistance of PASC materials prepared with different isocyanates: 5 dumbbell-shaped tensile splines (0.5 mm (T) × 2 mm (W) × 35 mm (L)) were selected and immersed in deionized water, soaked at 60 °C for 7 days; then the water on the surface of the sample was wiped off to test its mechanical properties with a tensile rate of 50 mm min^{-1}.

2.5 Solvent recycling and reprocessing of PASC-IPDI-IPDH-3

First, the cross-linked PASC-IPDI-IPDH-3 was cut into small pieces, and then the material was placed in a dumbbell-shaped mold for hot pressing at a certain temperature and pressure. Subsequently, the material was cooled to RT and taken out for tensile testing.

The solvent recycling process of the material is as follows: first, 6 g of PASC-IPDI-IPDH-3 material was added in 50 mL DMF, and stirred at 100 °C until dissolved; then the solution was poured into a mold, dried at 80 °C for 24 h, pumped at 100 °C and vacuum dried for 48 h. Finally, the dumbbell-shaped stretch samples were cut for tensile testing. The above recycling process was repeated 4 times. The recycling efficiency (ν) is calculated using the equation:

$$\nu = \frac{\sigma_r}{\sigma_0} \times 100\%$$

where σ_r represents the stress at break of the recycled material and σ_0 represents the stress at break of the initial material.

2.6 Preparation of PASC-IPDI-IPDH-3/CF composites

First, a certain molar ratio of IPDI, IPDH, and tri-HDI was added to DMF to obtain a clarified PASC-IPDI-IPDH-3 solution by

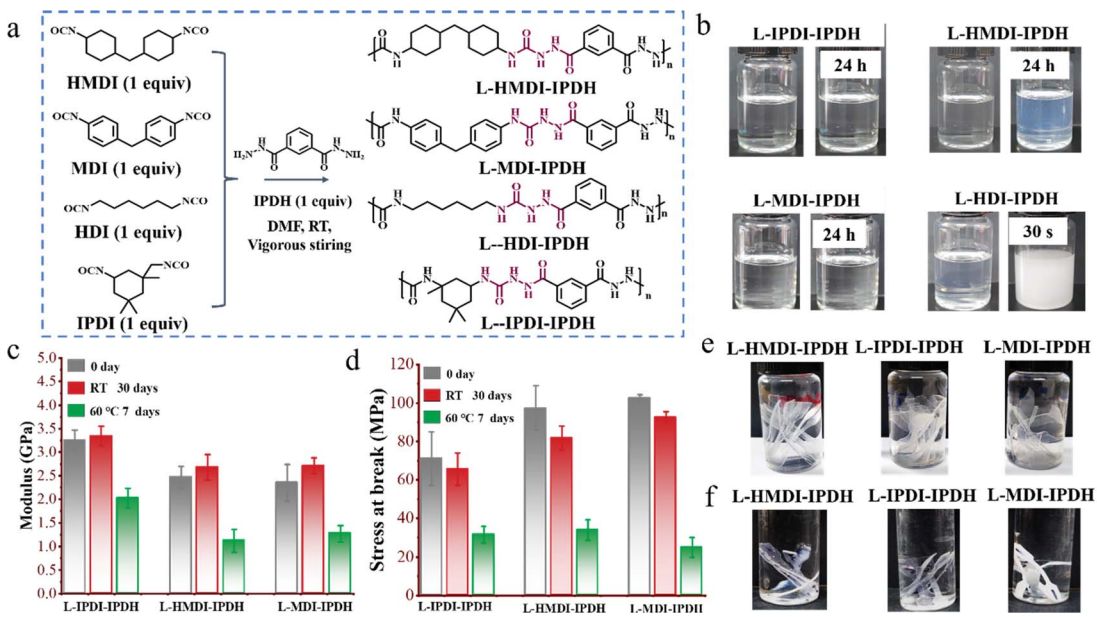

Fig. 1 (a) The chemical structure of PASC materials synthesized with different isocyanates. (b) Optical pictures of polymer solutions after the reaction of different isocyanates with IPDH. (c) and (d) The mechanical properties of different PASC materials. (e) An optical picture of the material after soaking at RT for 30 days. (f) An optical picture of the material after soaking at 60 °C for 7 days.

constant stirring, and then the polymer solution was poured into a mold containing carbon fibers. After the mold was dried at 100 °C for 24 h, the material was removed and hot pressed at 160 °C and 20 MPa for 2 min, and then vacuum dried at 100 °C for 48 h to obtain a uniform prepreg. Carbon fiber prepreg materials with different carbon fiber contents were prepared according to the above method, which were denoted as CFRP-60%, CFRP-50%, and CFRP-40%, the percentage of which is the mass fraction of carbon fiber in the composite material.

2.7 Preparation of carbon fiber composite laminates

Preparation of the flexural specimens of carbon fiber composites: two-layer prepregs were hot-pressed at 160 °C and 20 MPa for 10 min to obtain a double-layered composite laminate, which was then cut into 25 mm (L) × 10 cm (W) samples for flexural testing. Double-layer plates with different carbon fiber contents are denoted as 2-CFRP-60%, 2-CFRP-50%, and 2-CFRP-40%. The percentage is the mass fraction of carbon fiber in the composite material.

The short beam shear (SBS) test samples were prepared by hot pressing 20 layers of CFRP-50% carbon fiber prepreg at 160 °C under different pressures (5 MPa, 10 MPa, 20 MPa, and 30 MPa) for 10 min.

3. Results and discussion

3.1 The influence of different isocyanates on the properties of polyacylsemicarbazide

To investigate the effect of different isocyanates on the properties of PASC, we prepared PASC with different isocyanates by the reaction of IPDI/HMDI/HDI/MDI with IPDH, as shown in Fig. 1a. IPDH reacted completely with isocyanate to form a homogeneous and transparent solution (Fig. 1b). It is worth noting that the L-HDI-IPDH solution gradually became cloudy, showing macroscopic phase separation and precipitation, and failed to form a complete material. However, the PASC solutions prepared with HMDI, IPDI, and MDI were still homogeneous and transparent after standing for 24 hours. This phenomenon may be due to the linear polymer chains and good flexibility formed by HDI, and the resulting strong hydrogen bonding interaction of ASC groups, which make the molecular chains aggregate and induce macroscopic phase separation. The structure of the as-synthesized polymers was confirmed by ^{1}H NMR as shown in Fig. S1.† The mechanical properties of PASC prepared from different isocyanates are shown in Fig. 1c and d. It can be seen that all of them show excellent mechanical properties (see Table S1† for specific data). L-IPDI-IPDH not only exhibits excellent mechanical properties but also shows a great Young's modulus of 3.3 GPa, which is much higher than that of L-HMDI-IPDH (2.4 ± 0.2 GPa) and L-MDI-IPDH (2.3 ± 0.4 GPa). Meanwhile, the molecular weights of all materials tested by GPC are less than 20 000 (Table S1†), which strongly indicates that the outstanding mechanical properties of PASC materials are related to the strong hydrogen bonding interaction of ASC in their structure.

Materials are often exposed to different humidity environments in practical applications, so the water resistance of materials is very important. We used GB T 2573-2008 as a measurement standard to characterize the high temperature water resistance of the material. First, we immersed the PASC material in deionized water at 60 °C for 7 days. It can be seen that the material will appear a little white after soaking due to water erosion (Fig. 1f shows the appearance of PASC material after soaking). Subsequently, the water on the surface of the material was wiped off and the tensile test was performed. The test results are shown in Fig. 1c and d. After all the samples were soaked at 60 °C for 7 days, the mechanical strength and Young's modulus decreased. The Young's modulus and tensile strength of L-IPDI-IPDH are 62% (2.1 ± 0.2 GPa) and 44.3% (31.5 ± 4.3 MPa) of the initial value (Table S1, ESI†), respectively, showing optimal high temperature and water resistance. To further characterize the water resistance of the material at RT, the material was soaked in deionized water at RT for 30 days. As shown in Fig. 1e, the appearance of all materials did not change significantly even after 30 days of soaking at RT. Then, the water on the surface of the sample was wiped off and its mechanical properties were measured. The results are shown in Fig. 1c and d; the mechanical properties of all materials did not change significantly, exhibiting excellent RT water resistance. Meanwhile, we compared this work with our previous work[33] and it can be seen that the PASC material prepared with aliphatic ADH was only soaked in water for 24 h, and its mechanical properties decreased by 44% (Fig. S2a,† Table 1). Such results prove that the introduction of rigid groups and strong hydrogen bonding can improve the mechanical properties of the material while improving the water resistance of the material. The hydrophobicity of the material was further characterized by the water contact angle experiment, and the experimental results are shown in Fig. 2a. The data suggest that L-IPDI-IPDH possesses

Table 1 The mechanical properties of PASC materials with different crosslinking indices

Sample	Initial modulus (GPa)	Stress at break (MPa)	Strain at break (%)
L-IPDI-IPDH	3.3 ± 0.2	71.1 ± 14.1	2.7 ± 0.5
PASC-IPDI-IPDH-1	3.6 ± 0.2	82.1 ± 14.7	2.5 ± 0.4
PASC-IPDI-IPDH-3	4.1 ± 0.4	97.6 ± 12.1	2.8 ± 0.5
PASC-IPDI-IPDH-5	3.6 ± 0.4	75.8 ± 10.2	2.3 ± 0.4
PASC-IPDI-IPDH-7	3.2 ± 0.4	61.9 ± 10.8	2.9 ± 0.3
E51/MPD	1.6 ± 0.1	83.2 ± 2.9	7.7 ± 0.5
Polyurea-3	2.3 ± 0.2	63.8 ± 8.2	3.6 ± 0.7

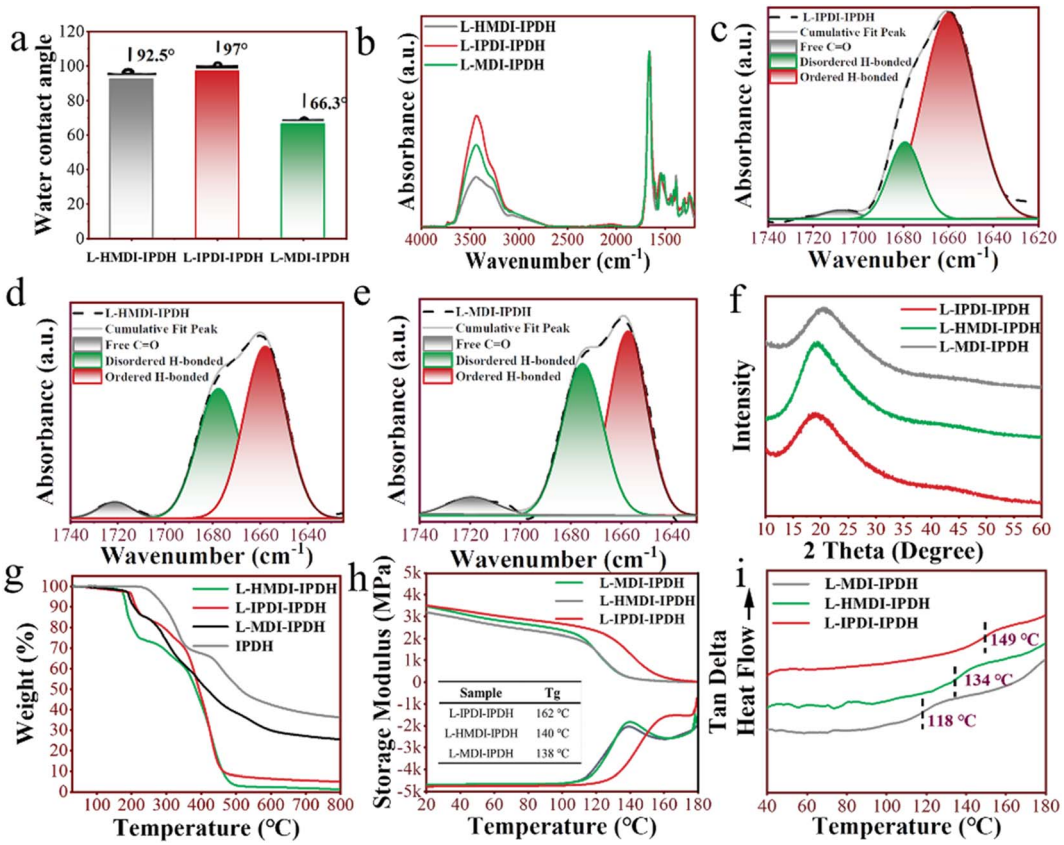

Fig. 2 (a) The water contact angle test of the material. (b) FTIR spectra of different PASC materials. (c), (d) and (e) Sub-peak fitting of C=O infrared characteristic peaks in different PASC materials. (f) XRD, (g) TGA, (h) DMA and (i) DSC curves of different PASC materials.

higher hydrophobicity. This difference may be related to the strong hydrogen bonding structure formed by different isocyanates in the ASC moieties.

The influence of different isocyanates on the internal hydrogen bonds of the material was studied by FTIR. The infrared spectroscopy test results of different samples are shown in Fig. 2b. It can be seen that the 2260 cm^{-1} characteristic peak attributed to –NCO in all samples disappeared, proving that all isocyanates reacted successfully with IPDH.[34,35] Fig. S2b† shows the changes in the absorption peaks of C=O in different samples. The absorption peaks of C=O in L-IPDI-IPDH, L-HMDI-IPDH and L-MDI-IPDH are at 1659 cm^{-1}, 1665 cm^{-1} and 1682 cm^{-1}, respectively. This phenomenon is caused by the different internal hydrogen bond interactions of different PASC materials.[36,37] To further study the effect of different isocyanates on the hydrogen bonding structure of PASC materials, we deconvolved the C=O characteristic absorption peaks of different materials and fitted the Gauss-Lorentz splitting of the FTIR spectrum, as shown in Fig. 2c–e. The deconvoluted subpeak can be assigned to the free and H-bonded C=O in the FTIR C=O absorption bands.[34,38] Quantitative analysis shows that the hydrogen-bonded C=O ratios in L-IPDI-IPDH, L-HMDI-IPDH, and L-MDI-IPDH are 97.9%, 95.9%, and 93.6%, respectively, suggesting that all samples exhibit very strong hydrogen bonding interactions (Table S2, ESI†). The proportion of hydrogen-bonded C=O in the material is defined as the percentage of C=O peaks bound by hydrogen bonds over the total C=O peak area. It is worth noting that the proportion of ordered hydrogen bonds in the C=O characteristic peaks of L-IPDI-IPDH is 81.5%, which is much higher than those of L-HMDI-IPDH (57.2%) and L-MDI-IPDH (53.2%). The proportion of ordered hydrogen bonds in the material is defined as the percentage of C=O peaks bound by ordered hydrogen bonds over the total C=O peak area. This difference may be due to the fact that aliphatic IPDI and HMDI are more flexible than aromatic MDI and easily form hydrogen bonds in the molecular chain. However, compared with HMDI, IPDI has poor symmetry due to its two isocyanate (NCO) groups that have different reactivities, whereas the secondary NCO group with a lower steric resistance effect is more reactive in the absence of a catalyst. This unique chemical structure makes it useful to control the structure of materials in polymer synthesis. Therefore, the proportion of C=O ordered hydrogen bonds in L-IPDI-IPDH is much higher than that in L-HMDI-IPDH. It may be that a large number of ordered hydrogen bond structures in L-IPDI-IPDH provide the material with excellent water resistance.

3.2 Mechanical and thermal properties of PASC-IPDI-IPDH with different cross-linking indices

We selected IPDI, IPDH, and tri-HDI to prepare dynamic crosslinked polymers with different crosslinking indices

(Fig. 3a), and their mechanical properties are shown in Fig. 3b (the specific data are shown in Table 1). When the cross-linking index is 3, PASC-IPDI-IPDH-3 has the best mechanical properties. Its Young's modulus reaches 4.1 ± 0.4 GPa, and its tensile strength reaches 97.6 ± 12.1 MPa, showing excellent mechanical properties. These results can be explained as follows: because ultrahigh dynamic bond content and strong hydrogen-bonding strength are synergistically introduced into the polymer network with covalent cross-linking, the optimized sample PASC-IPDI-IPDHI-3 exhibits excellent mechanical properties. Further increasing the covalent cross-linking index to 5 or more will lead to excessive polymer chain interactions and linking, and result in brittleness of the materials. To the best of our knowledge, the outstanding mechanical properties of PASC-IPDI-IPDH-3 almost surpass those of the high-performance dynamic polymers reported so far (shown in Fig. 3c). To further compare the differences in the mechanical properties of PASC-IPDI-IPDH-3 possessing strong internal hydrogen bonds with those of conventional epoxy resins and structurally similar polyurea, we used isophenylenediamine (MPD) to cure E51 resin to prepare a conventional epoxy resin (E51/MPD), and isophenylenediamine (IPDA) to prepare polyurea with the same crosslinking index (PA-3). Fig. 3d shows the mechanical properties of PASC-3 and conventional epoxy and PA-3. It can be seen that the mechanical properties of PASC-IPDI-IPDH-3 are significantly higher than that of conventional epoxy resins and PA-3 (see Table 1 for specific data), which are similar in structure but have a weaker hydrogen bond interaction. Such outstanding mechanical properties are mainly attributed to the synergy effect of the chemical cross-linking and strong physical cross-linking hydrogen bonds within PASC. The T_g of materials with different crosslinking indices was characterized by DMA. It can be seen that with the increase in crosslinking degree, the T_g of the material gradually increases; specifically the T_g of PASC-IPDI-IPDH-3 is 174 °C. DSC testing of PASC materials with different crosslinking indices also showed the same trend.

3.3 Dynamics of the PASC-IPDI-IPDH-3 material

In our previous work,[32] the dynamic dissociation of ASC moieties' can be achieved in a unimolecular fashion upon lengthening of the appropriate C–N bond and a concomitant proton transfer from the –NH group to another one, accompanied by

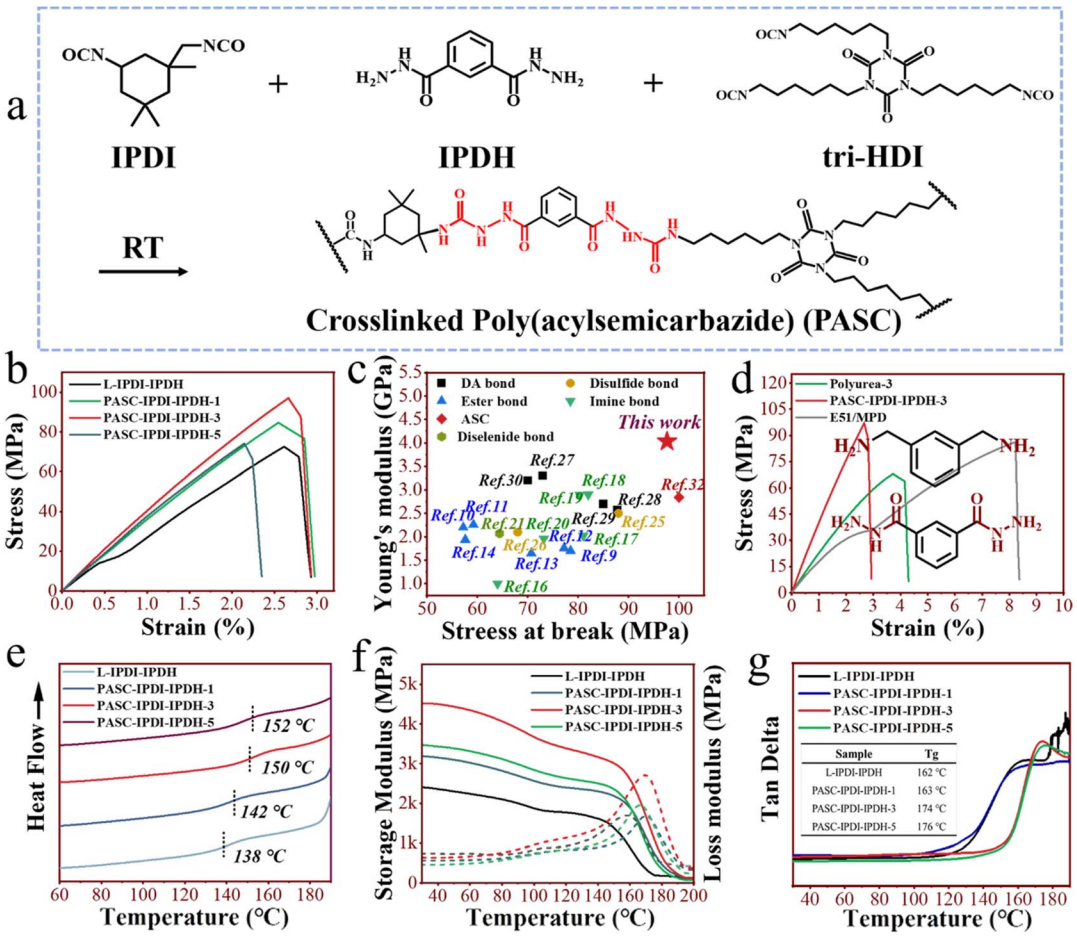

Fig. 3 (a) The synthetic route of the cross-linked PASC materials. (b) The mechanical properties of PASC materials with different cross-linked indices. (c) Comparison chart of the mechanical properties of PASC-IPDI-IPDH-3 and the current dynamic polymer. (d) The mechanical properties of PASC-IPDI-IPDH-3, MPD-cured E51, and polyurethane 3 materials with the same crosslinking index. (e) DSC curve and DMA curve (f) and (g) of PASC materials with different cross-linking indices.

the generation of the constituent hydrazide and isocyanate (Fig. 4a). We observed the infrared spectra of L-IPDI-IPDH and ordinary polyurea L-IPDI-IPDA with temperature changes through temperature-dependent infrared spectroscopy (Fig. 4b and c). It can be seen that as the temperature increases from 30 °C to 160 °C, the characteristic peaks belonging to the –NCO group gradually appear at 2260 cm^{-1}, but the appearance of-NCO characteristic peaks are not observed in ordinary polyurea L-IPDI-IPDA. The emergence of this phenomenon intuitively proves the dynamic dissociation mechanism of PASC. We also demonstrated the dynamic exchange reaction of ASC groups through ^1H NMR (Fig. S3†) by heating the mixture of 2-benzoyl-*N*-cyclohexylhydrazine-1-carbamide and 4-methoxybenzoylhydrazine (molar ratio 1 : 1) at 120 °C for different durations of time. Furthermore, we characterized the dynamics of the crosslinked material through reprocessing experiments. Fig. 4d shows that the powdered PASC can form a complete dumbbell-shaped spline after 10 min of hot pressing at 160 °C and 20 MPa, which strongly proves the dynamics of the network. We characterized the mechanical properties of the material under different reprocessing conditions around the material T_g (DSC, 153 °C) (Fig. 4f). The specific mechanical properties of the material under different processing conditions are shown in Table 2. It can be seen that PASC-IPDI-IPDH-3 showed the best mechanical properties after hot pressing at 160 °C and 20 MPa for 10 min. Specifically, Young's modulus, mechanical strength, and elongation at the break of the material can recover 78.1% (3.1 ± 0.1 GPa), 96.1% (89.6 ± 10.3 MPa), and 114% (3.3 ± 0.6) of the initial properties, respectively. To more intuitively demonstrate the stability and reversibility of the crosslinking network in PASC-IPDI-IPDH-3, we characterized the multiple solvent recovery capacity of the material in DMF. Fig. 4e shows the solvent recovery process of the material. It can be seen that PASC-IPDI-IPDH-3 only swells and does not dissolve in DMF at RT for 24 h, and then the material is heated at 100 °C for 2 h to form a homogeneous solution. This phenomenon intuitively confirms the thermal reversibility of the internal cross-linked network of PASC-IPDI-IPDH-3. The recycled PASC-IPDI-IPDH-3 solution was poured into a PTFE mold and dried to form a complete material. Young's modulus, tensile strength, and elongation at break of the recycled materials are 4.1 ± 0.4 GPa, 110.9 ± 23.2 MPa, and 3.4 ± 0.8%, respectively. Using the same

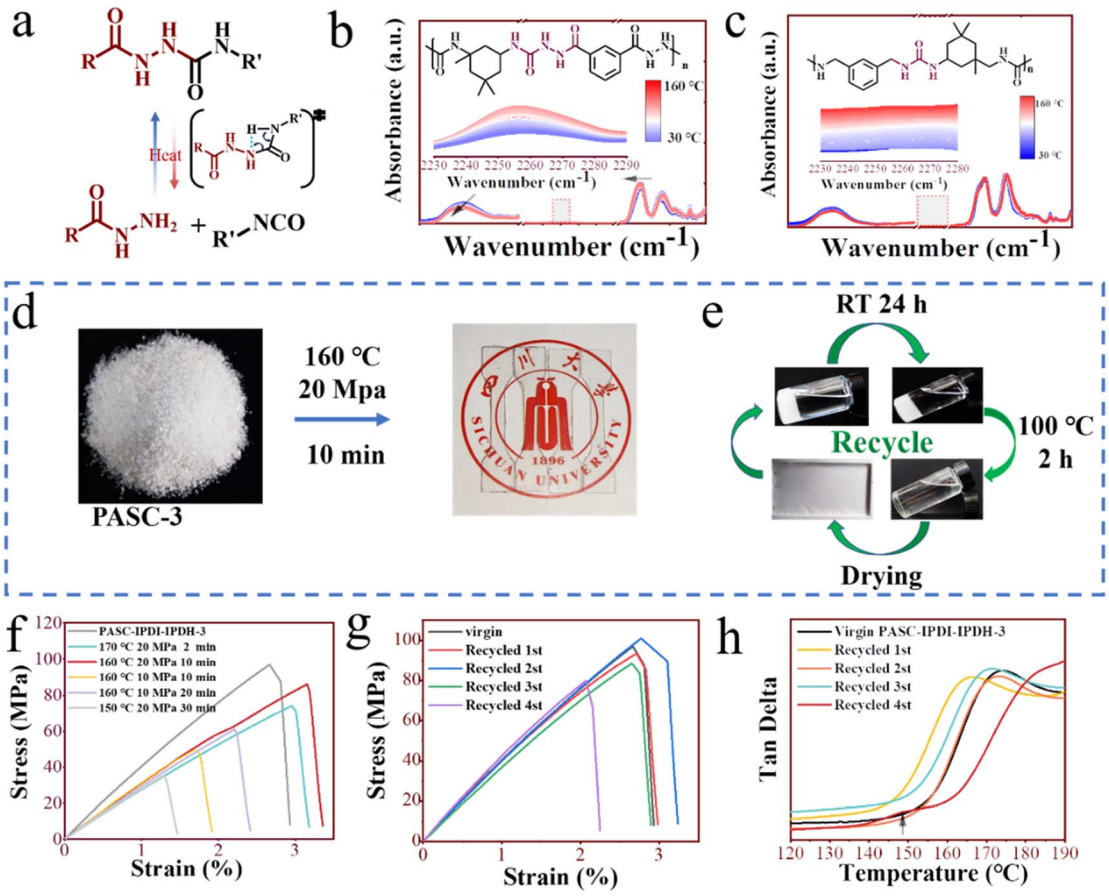

Fig. 4 (a) Schematic diagram of the dissociation exchange of ASC groups. (b) and (c) are the temperature-dependent infrared spectroscopy curves of L-IPDI-IPDH and L-IPDI-IPDA, respectively. (d) An optical picture of the reprocessing of the PASC-3 material. (e) Schematic picture of solvent recycling of PASC-3. (f) The mechanical properties of materials under different reprocessing conditions. (g) Changes in the mechanical properties of the material after repeated recovery in DMF at 100 °C four times. (h) The DMA test curves of the material after solvent recycling four times.

Table 2 Mechanical properties of PASC-IPDI-IPDH-3 under different reprocessing conditions and after multiple solvent recoveries

Sample	Initial modulus (Gpa)	Stress at break (Mpa)	Strain at break (%)	Recycling efficiency (%)
PASC-IPDI-IPDH-3	4.1 ± 0.2	93.3 ± 12.9	2.8 ± 0.5	
170 °C, 20 MPa, 2 min	2.8 ± 0.2	72.6 ± 1.6	2.9 ± 0.1	77.9
160 °C, 20 MPa, 10 min	3.1 ± 0.1	89.6 ± 10.3	3.3 ± 0.6	96.1
160 °C, 10 MPa, 10 min	3.1 ± 0.6	54.6 ± 6.3	2.0 ± 0.6	58.6
160 °C, 10 MPa, 20 min	3.0 ± 6.5	61 ± 3.5	2.2 ± 4.3	65.4
150 °C, 20 MPa, 30 min	2.8 ± 0.1	35.1 ± 0.3	1.3 ± 0.1	37.5
Recycled 1st	4.1 ± 0.4	110.9 ± 23.2	3.4 ± 0.8	113.6%
Recycled 2nd	4.2 ± 0.3	88.9 ± 10.4	2.3 ± 0.4	91.1%
Recycled 3rd	4.3 ± 0.3	85.3 ± 20.8	2.6 ± 0.4	87.3%
Recycled 4th	4.4 ± 0.3	75.9 ± 7.4	2.2 ± 0.6	77.8%

method, even after repeating the solvent cycle four times, the material still exhibits mechanical properties comparable to those of the pristine material (Fig. 4g). DMA was used to characterize the thermodynamic properties of the material after multiple cycles (Fig. 4h). The test results show that the thermodynamic properties of the material after three cycles of reprocessing do not change significantly, but in the fourth recycling of DMA, a small peak appeared at about 150 °C, which may be related to the partial side reaction of isocyanate during the recycling process.

The stability of the internal crosslinking network of the polymer has a very important impact on the service life and dimensional stability of the material.[8,39] Therefore, to further characterize the stability of the internal crosslinking network of PASC materials, we characterized the room temperature stability of PASC-IPDI-IPDH-3 in conventional solvents. As shown in Fig. S4,† the material was immersed in conventional solvents such as AC, THF, DMF, water, ethanol, and DMSO for 24 hours, and the swelling ratio of the material was measured. It can be seen that all materials can maintain their original shape after being soaked in low-polarity H_2O, EtOH, THF, and acetone for 24 h, and then the swelling of the materials is less than 1% (Fig. 5a–c), showing excellent solvent resistance. It is worth noting that even in strongly polar solutions DMF and DMSO, PASC-IPDI-IPDH-3 only swells and does not dissolve. This phenomenon suggests that the dynamic crosslinking polymer network has good stability in the solvent at RT. To further characterize the stability of the internal crosslinking network of the material, we used DMA to characterize the creep behavior test of the crosslinked polymer at different temperatures. The test results are shown in Fig. 5d. It can be seen that the material does not show creep behavior at 25 °C and exhibits similar behavior to ordinary elastomers. With the increase in temperature, the elastic deformation and viscous deformation of the material gradually increase. It should be noted that after the stress is removed from the material at 120 °C, the strain of the

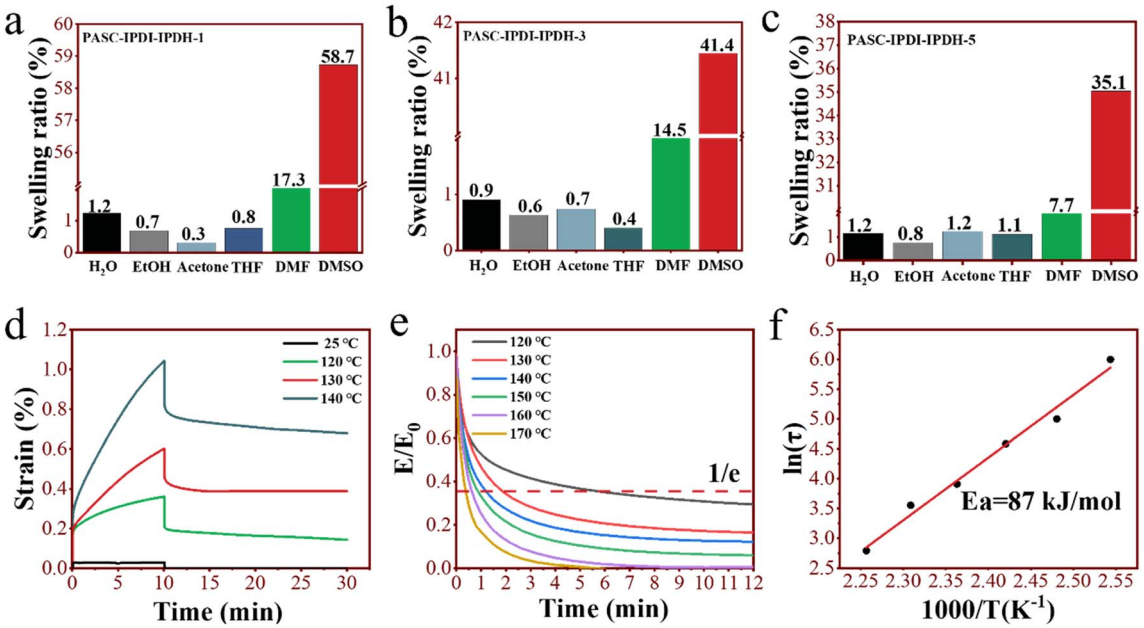

Fig. 5 The swelling ratio of (a) PASC-1, (b) PASC-3 and (c) PASC-5. (d) The creep curve and (e) the stress relaxation curves of PASC-3 at different temperatures. (f) The Arrhenius plot of the measured relaxation times from the frequency sweep experiments.

material can recover by 88%, showing a certain high temperature creep resistance behavior.

To further characterize the dynamics of the cross-linked network inside the material, we investigated PASC-IPDI-IPDH-3 by stress relaxation experiments. Fig. 5e shows the stress relaxation curves of the material at different temperatures. It can be seen that the stress of the material cannot be relaxed to zero in the temperature range of 120–150 °C, which suggests the characteristics of ordinary thermosetting materials. This phenomenon confirms the formation of an internal cross-linking structure. However, with the increase in temperature, the relaxation time of the material is gradually accelerated. When the temperature is 170 °C, the material can relax to zero within 6 min. The appearance of this phenomenon strongly proves the reversibility of the internal cross-linking structure of the material. The Maxwell model is used to describe the relaxation behavior of the material, and the relaxation time is defined as the relaxation time of the material modulus to 1/e of the initial modulus. The fitted data are shown in Fig. 5f, and its relaxation activation energy is 87 kJ mol^{-1}.

3.4 Preparation and characterization of PASC-3-carbon fiber composites

Based on the excellent mechanical properties and solvent recycling ability of the PASC-IPDI-IPDH-3 material, we used it as the material matrix to prepare carbon fiber composites with different resin contents. The preparation process of the composite material is shown in Fig. 6a. First, a certain amount of IPDI, IPDH, and tri-HDI are added to DMF and stirred until the solution becomes clear; then the solution is poured into a mold containing carbon fibers, dried to obtain a single layer of CFRP prepreg, and then the multi-layer prepreg is pressed into a multi-layer carbon fiber composite material at the appropriate temperature and pressure. Fig. 6b and c show the SEM images of the surface and cross-section of the CFRP-50% prepreg, and it can be seen that the resin is uniformly attached to the fiber surface, showing good wettability. To study the influence of resin content on the performance of composite materials, we prepared prepreg materials of CFRP-60%, CFRP-50%, and CFRP-40%, where the percentage represents the mass fraction of carbon fibers in the weight of the total composite material, and characterized them through tensile tests. Fig. 6d shows the mechanical properties of carbon fiber prepregs with different resin contents (see Table S3† for specific data). It can be seen that with the increase in resin content, the mechanical properties of the material gradually decrease. Among them, the tensile strength and modulus of CFRP-50% prepreg are 378.1 ± 38.4 MPa and 37.7 ± 5.0 GPa, respectively. Three-point bending is used to characterize the flexural strength of the double-layer composite material (Fig. 6e). The flexural strength of the composite material increases first and then decreases with the increase in resin content. This phenomenon can be explained as follows: on the one hand, when the resin content is low, the composite material layer cannot be well combined with the layer, resulting in lower bending strength of the material. On

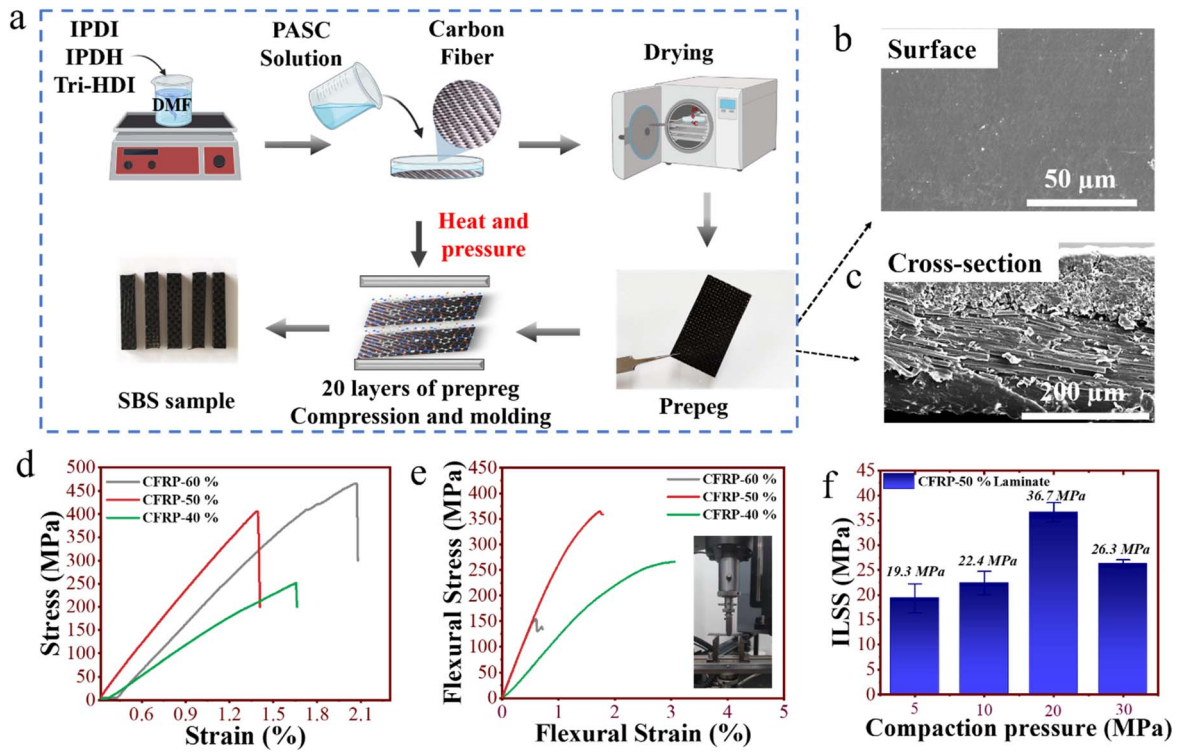

Fig. 6 Schematic illustration of the preparation of the PASC-3/CF carbon fiber composite material. (b) and (c) SEM of CFRP-50% carbon fiber prepreg. (d) and (e) The mechanical properties and bending properties of carbon fiber composite materials with different resin contents. (f) ILSS of 20 laminates prepared at different hot pressing pressures.

the other hand, when the resin content is too high, the fiber fraction decreases and the enhancement effect weakens. The specific data of composite materials are shown in Table S4.† The flexural strength and modulus of CFRP-50% are 326.9 ± 37.4 MPa and 29.8 ± 2.1 GPa, respectively. Based on the mechanical properties of the prepreg and the bending strength of the double-layer laminate, we selected a composite material with a resin content of 50% for further study.

We selected 20 layers of CFRP-50% prepreg to prepare SBS samples by hot pressing at 160 °C for 10 min under different pressures and explored the effect of hot-pressing pressure on the interlaminar shear strength (ILSS) of SBS samples. As shown in Fig. 6f, with the increase in hot-pressing pressure, the ILSS of the composites show a trend of increasing first and then decreasing. This phenomenon can be explained as the increase in pressure will contribute to the binding between the prepreg layers; however, with the further increase of pressure, the resin between the composite laminates will be squeezed out too much which is not conducive to the binding between the layers. Therefore, the appropriate pressure has a very important influence on the bonding between the composite layers. Specifically, when the pressure is 20 MPa, the carbon fiber composite material has an optimal ILSS of 36.7 MPa.

3.5 Healing and recycling properties of the CFRP-50% composite

In the application process of traditional carbon fiber composite materials, small defects are often caused by external forces, which have a huge impact on the stability and safety of composite materials. At the same time, traditional thermosetting carbon fiber composite materials (such as epoxy resins) fail to recycle carbon fibers and resins due to their insoluble and non-fusible properties. Therefore, endowing composites with self-healing properties and mild recyclability has profound implications for a sustainable economy. To evaluate the self-healing ability of carbon fiber composite materials when the interior is damaged, we use the samples of the tested ILSS to repair under certain conditions and then test the ILSS again. Fig. 7a shows the ILSS before and after the composite material is repaired. It can be seen that after the composite material is repaired by hot pressing, the ILSS (25.9 MPa) can return to 70.6% of its initial value.

We further characterized the resin and carbon fiber recycling capabilities of composite materials through solvent recycling. First, we investigated the recycling process of resin and carbon fibers for CFRP-50% prepreg. Fig. 7c shows the weight loss curve of CFRP-50% prepreg at different recovery times in DMF at 100 °C. It can be seen that after 140 min of recycling in DMF at 100 °C, carbon fibers and resin can achieve nearly 100% recovery. Fig. 7b shows the changes in the morphology of the surface of the carbon fiber of the composites at different solvent recovery times. It can be seen that the CFRP-50% prepreg after being soaked in DMF for 24 h at RT and the surface of the material became rough due to the swelling effect of DMF. However, on increasing the soaking time in DMF at 100 °C, the resin on the surface of carbon fibers gradually dissolves completely. Fig. 7d–f show the XRD, XPS, and XRD curves of carbon fibers before and after recycling, respectively. The results show that the structure of the carbon fiber has not changed significantly before and after recycling. Meanwhile, the mechanical and thermodynamic properties of the recycled resin were characterized by tensile testing and DMA (Fig. 7g and h), which shows that the recycled resin still retains the initial properties. Subsequently, we used the recycled resin and carbon fibers to re-prepare the carbon fiber prepreg and characterized the mechanical properties of the prepreg before and after recovery through tensile testing (Fig. 7i). The results show that the recycled prepreg still has the same initial performance.

To further characterize the solvent recycling performance of multilayer composite laminates, we performed closed-loop recovery of PASC resin and carbon fibers using 10-layer CFRP-50% laminates, and the specific recovery process is described in the experimental section. Fig. 7j shows the optical image of the carbon fiber and resin recovered from the 10-layer CFRP-50% laminate. It can be seen that the complete carbon fiber and PASC resin can be successfully recovered using the solvent recycling method, and then the recycled resin carbon fiber is recombined. The ILSS of the recycled material was characterized by three-point bending, as shown in Fig. 7k; the ILSS of the recycled CFRP-50 laminate is 30.2 MPa, 82.3% of the original value, showing a very good solvent recycling ability. Overall, the solvent recycling experiments of carbon fiber composite materials show that the carbon fiber composite materials we prepared have excellent solvent recovery capabilities and can achieve nearly 100% non-destructive recovery of carbon fibers and resin.

The mechanism of fully recyclable composite materials is discussed as follows. The ASC moieties are one kind of dissociative dynamic bonds, which can be cleaved into the constituent reactive partners hydrazide and isocyanate in a unimolecular fashion upon lengthening of the appropriate C–N bond and a concomitant proton transfer from an –NH group to another one.[32] The reversible dissociation of ASC moieties enables the decrosslinking of the PASC-IPDI-IPDH-3 network and subsequently leads to the complete dissolution of the resin of the composite material. Therefore, the insoluble carbon fiber can be readily separated from the dynamic polymer solution in a non-destructive way, allowing the full recycling of the composite materials with no obvious decrease in overall performances.

Before concluding this work, we wish to briefly explain the innovations in the structural design that distinguishes or differentiates the present study from our previous studies.[32,33] In our previous work,[32] we proposed and studied the dynamics of ASC groups and their dynamic mechanisms for the first time. In this work, ultrahigh dynamic bond content and strong hydrogen-bonding strength are elaborately introduced into the synthesized PASC materials through the reaction of IPDI/IPDH and tri-HDI without using long chain extenders as soft segments. This unique chemical structure makes its mechanical properties exceed those of the currently reported dynamic polymers and conventional epoxy resins, while still maintaining good dynamics. In our another study,[33] we used aliphatic ADH

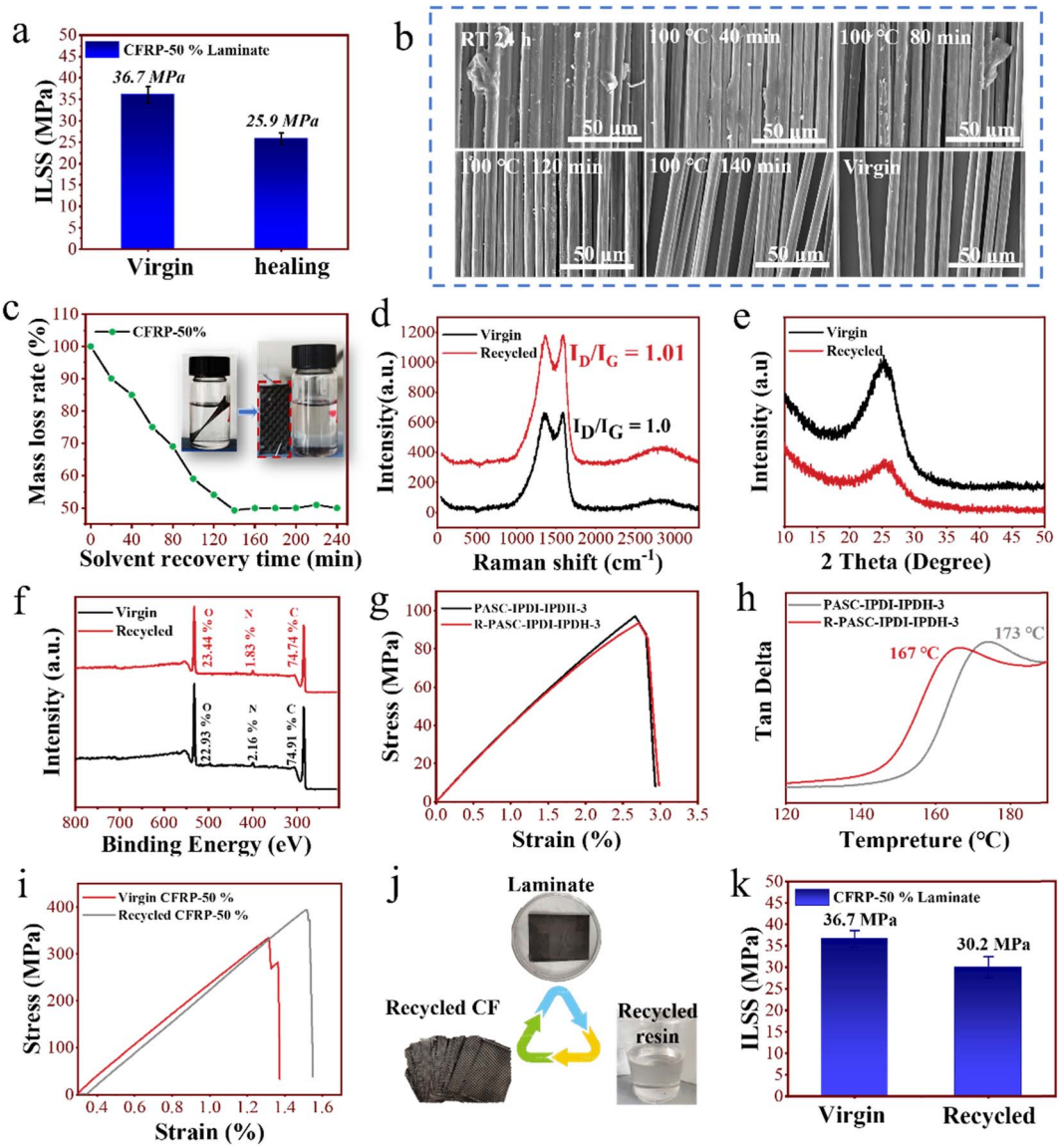

Fig. 7 (a) The ILSS self-repairing performance of the 20-layer carbon fiber laminate. (b) SEM of CFRP-50% prepreg with different solvent recycling times. (c) The solvent recycling curve of CFRP-50% prepreg. (d) Raman spectroscopy, (e) XRD, and (f) XPS spectra of the carbon fiber after solvent recycling. The mechanical properties (g) and thermodynamic properties (h) of the resin after solvent recovery.(i) The mechanical properties of the regenerated CFRP-50% prepreg. (j) Optical pictures of the 10-layer carbon fiber laminate before and after recycling. (k) ILSS of the regenerated CFRP-50 laminate.

and HMDI to prepare a crosslinked PASC material with a tensile strength of 100 MPa, a Young's modulus of 2.8 GPa, and a T_g of 123 °C, and studied its application in carbon fiber composite materials. However, the water resistance of the material is so poor that the material can only maintain 56% of its original mechanical properties after being soaked in water at room temperature for 12 h (Fig. S2†). Meanwhile, the influence of the internal hydrogen-bonding structure on the PASC material properties has not been studied. In this work, by comparing the influence of different molecular structures on the hydrogen-bonding strength of PASC materials, IPDH with a rigid chemical structure (benzene rings) is chosen to prepare a PASC material with higher stiffness and stronger hydrogen bonding strength, which significantly improves the mechanical properties of the material and provides the material with excellent water resistance. Even after soaking in water at RT for 30 days, the PASC-IPDI-IPDH material still maintains 92.3% of its initial mechanical properties.

Besides, the introduction of a rigid structure (benzene ring of IPDH) and strong hydrogen bonding inside PASC significantly improve the mechanical properties and glass transition temperature of the material. The optimized sample PASC-IPDI-IPDHI-3 exhibits great mechanical strength with a Young's modulus of ~4.1 GPa, a stress at break of ~97.6 MPa, and shows good thermal properties with a T_g of ~174 °C. This study does report some significant results based on the rational new molecular structure design, which has provided a paradigm on how to achieve recycling of carbon fibers and polymer resin

from a CFRP composite and prepare a high strength dynamic covalent crosslinked polymer with great self-healing/recycling capability.

Conclusions

In summary, we prepared a novel dynamic crosslinked polymer with ultra-high mechanical properties that are significantly better than those of ordinary conventional epoxy resins. The carbon fiber reinforced composites of this dynamic polymer all show excellent solvent recycling ability, and can achieve nearly 100% non-destructive recovery of carbon fibers and the resin matrix. Specifically, the optimized sample PASC-IPDI-IPDHI-3 exhibits great mechanical strength with a Young's modulus of ~4.1 GPa, a stress at break of ~97.6 MPa, and shows good thermal properties with a T_g of ~174 °C. The reversible dissociation/association of the dynamic ASC moieties provides the material with good reprocessing capacity and multiple solvent recovery capacity at high temperatures, enabling almost fully recovery of the mechanical properties of the reprocessed/recycled materials. Furthermore, we used PASC-IPDI-IPDH-3 to successfully prepare a carbon fiber reinforced composite material and systematically studied the influence of resin content and processing conditions on the performance of the composite material, and the ILSS of the optimized composite material reached 36 MPa. The healing efficiency of the composite evaluated with ILSS can reach up to 70.6%. The introduction of the dynamic crosslinked polymer PASC-IPDI-IPDH-3 can achieve nearly 100% closed-loop non-destructive recovery of resin and carbon fibers in carbon fiber composite materials. The regenerated carbon fiber composite material still has an initial ILSS of 82.3%. This work provides a new strategy for the preparation of high-strength and high-modulus dynamic polymer/carbon fiber composite materials, which can effectively alleviate the increasingly serious environmental problems caused by the failure of carbon fiber composite materials, so as to achieve the circular green development of carbon fiber composite materials.

Conflicts of interest

The authors declare that they have no known competing financial interests or personal relationships that could have appeared to influence the work reported in this paper.

Acknowledgements

We gratefully acknowledge the financial support from the National Natural Science Foundation of China (U20A20258) and Chengdu Municipal Bureau of Science and Technology (2022-YF05-00183-SN).

References

1 L. C. Bank, F. R. Arias, A. Yazdanbakhsh, T. R. Gentry, T. Al-Haddad, J.-F. Chen and R. Morrow, *Recycling*, 2018, **3**, 3.
2 Y. Li, B. Zhou, G. Zheng, X. Liu, T. Li, C. Yan, C. Cheng, K. Dai, C. Liu, C. Shen and Z. Guo, *J. Mater. Chem. C*, 2018, **6**, 2258–2269.
3 Y. Y. Liu, F. Lu, J. J. Wan, L. Yang, Y. D. Huang and Z. Hu, *Polym. Chem.*, 2022, **13**, 3063–3075.
4 J. Zhang, V. S. Chevali, H. Wang and C.-H. Wang, *Compos. B. Eng.*, 2020, **193**, 108053.
5 Y. Wan and J. Takahashi, *J. Compos. Sci.*, 2021, **5**, 86.
6 Y. Liu, Z. Yu, B. Wang, P. Li, J. Zhu and S. Ma, *Green Chem.*, 2022, **24**, 5691–5708.
7 G. Oliveux, L. O. Dandy and G. A. Leeke, *Prog. Mater. Sci.*, 2015, **72**, 61–99.
8 G. M. Scheutz, J. J. Lessard, M. B. Sims and B. S. Sumerlin, *J. Am. Chem. Soc.*, 2019, **141**, 16181–16196.
9 X. Kuang, Y. Zhou, Q. Shi, T. Wang and H. J. Qi, *ACS Sustain. Chem. Eng.*, 2018, **6**, 9189–9197.
10 Y. Xu, H. Zhang, S. Dai, S. Xu, J. Wang, L. Bi, J. Jiang and Y. Chen, *Compos. Sci. Technol.*, 2022, **228**, 109676.
11 W. Li, L. Xiao, J. Huang, Y. Wang, X. Nie and J. Chen, *Compos. Sci. Technol.*, 2022, **227**, 109575.
12 C. Hao, T. Liu, W. Liu, M.-e. Fei, L. Shao, W. Kuang, K. L. Simmons and J. Zhang, *J. Mater. Chem. A*, 2022, **10**, 15623–15633.
13 Y. Xu, S. Dai, H. Zhang, L. Bi, J. Jiang and Y. Chen, *ACS Sustain. Chem. Eng.*, 2021, **9**, 16281–16290.
14 S. Wang, S. Ma, Q. Li, X. Xu, B. Wang, W. Yuan, S. Zhou, S. You and J. Zhu, *Green Chem.*, 2019, **21**, 1484–1497.
15 S. Wang, X. Xing, X. Zhang, X. Wang and X. Jing, *J. Mater. Chem. A*, 2018, **6**, 10868–10878.
16 P. Taynton, H. Ni, C. Zhu, K. Yu, S. Loob, Y. Jin, H. J. Qi and W. Zhang, *Adv. Mater.*, 2016, **28**, 2904–2909.
17 H. Memon, Y. Wei, L. Zhang, Q. Jiang and W. Liu, *Compos. Sci. Technol.*, 2020, **199**, 108314.
18 Y. L. Sun, X. X. Tian, H. P. Xie, B. R. Shi, J. H. Zhong, X. D. Liu and Y. M. Yang, *Polymer*, 2022, **258**, 125313.
19 Y. Wang, A. Xu, L. Zhang, Z. Chen, R. Qin, Y. Liu, X. Jiang, D. Ye and Z. Liu, *Macromol. Mater. Eng.*, 2022, **307**, 2100893.
20 X. Liu, E. Zhang, Z. Feng, J. Liu, B. Chen and L. Liang, *J. Mater. Sci.*, 2021, **56**, 15733–15751.
21 X. An, Y. Ding, Y. Xu, J. Zhu, C. Wei and X. Pan, *React. Funct. Polym.*, 2022, **172**, 105189.
22 D. Zhang, T. Xu, C. Li, W. Xu, J. Wang and J. Bai, *J. CO2 Util.*, 2019, **34**, 716–724.
23 A. Yamaguchi, T. Hashimoto, Y. Kakichi, M. Urushisaki, T. Sakaguchi, K. Kawabe, K. Kondo and H. Iyo, *J. Polym. Sci., Part A: Polym. Chem.*, 2015, **53**, 1052–1059.
24 X. Liu, Y. Li, X. Xing, G. Zhang and X. Jing, *Polymer*, 2021, **229**, 124022.
25 A. Ruiz de Luzuriaga, R. Martin, N. Markaide, A. Rekondo, G. Cabanero, J. Rodriguez and I. Odriozola, *Mater. Horiz.*, 2016, **3**, 241–247.
26 W. Post, A. Cohades, V. Michaud, S. van der Zwaag and S. J. Garcia, *Compos. Sci. Technol.*, 2017, **152**, 85–93.
27 A. M. Peterson, R. E. Jensen and G. R. Palmese, *Compos. Sci. Technol.*, 2011, **71**, 586–592.
28 Y. Heo and H. A. Sodano, *Compos. Sci. Technol.*, 2015, **118**, 244–250.

29 Y. Heo, M. H. Malakooti and H. A. Sodano, *J. Mater. Chem. A*, 2016, **4**, 17403–17411.
30 G. Fortunato, L. Anghileri, G. Griffini and S. Turri, *Polymers*, 2019, **11**, 1007.
31 Z. Wang, X. Lu, S. Sun, C. Yu and H. Xia, *J. Mater. Chem. B*, 2019, **7**, 4876–4926.
32 D. Fu, W. Pu, J. Escorihuela, X. Wang, Z. Wang, S. Chen, S. Sun, S. Wang, H. Zuilhof and H. Xia, *Macromolecules*, 2020, **53**, 7914–7924.
33 S. Wang, D. Fu, X. Wang, W. Pu, A. Martone, X. Lu, M. Lavorgna, Z. Wang, E. Amendola and H. Xia, *J. Mater. Chem. A*, 2021, **9**, 4055–4065.
34 C. Yu, M. Salzano de Luna, A. Russo, I. Adamiano, F. Scherillo, Z. Wang, X. Zhang, H. Xia and M. Lavorgna, *Adv. Mater. Interfaces*, 2021, **8**, 2100117.
35 D. H. Fu, W. L. Pu, Z. H. Wang, X. L. Lu, S. J. Sun, C. J. Yu and H. S. Xia, *J. Mater. Chem. A*, 2018, **6**, 18154–18164.
36 Z. Wang, M. Song, X. Li, J. Chen, T. Liang, X. Chen and Y. Yan, *Polymers*, 2022, **14**, 3517.
37 M. Yang, X. Lu, Z. Wang, G. Fei and H. Xia, *J. Mater. Chem. A*, 2021, **9**, 16759–16768.
38 Z. Li, Y.-L. Zhu, W. Niu, X. Yang, Z. Jiang, Z.-Y. Lu, X. Liu and J. Sun, *Adv. Mater.*, 2021, **33**, 2101498.
39 J. Zhang, C. Shang, Z. Yu, L. Wang, J. Tang and F. Huang, *Macromol. Rapid Commun.*, 2022, **43**, 2100236.